

THE MOST PROBABLE CAUSE FOR THE HIGH GAMMA-RAY POLARIZATION IN GRB 021206

JONATHAN GRANOT

Institute for Advanced Study, Olden Lane, Princeton, NJ 08540; granot@ias.edu

Draft version September 23, 2018

ABSTRACT

The exciting detection of a very high degree of linear polarization, $P = 80\% \pm 20\%$, in the prompt γ -ray emission of the recent GRB 021206, provides strong evidence that synchrotron emission is the dominant radiation mechanism. Besides this immediate implication, there were also claims that this implies a magnetic field that is ordered on large scales within the ejecta, and must therefore be produced at the source, which in turn was used as an argument in favor magnetic fields playing an active role in the production of GRB jets. However, an alternative explanation was also suggested: a very narrow jet, of opening angle $\theta_j \sim 1/\gamma$, where $\gamma \gtrsim 100$ is the Lorentz factor during the GRB, viewed slightly outside its edge, at $\theta_j < \theta_{\text{obs}} \lesssim \theta_j + 1/\gamma$. This explanation also works with a magnetic field that is generated in the internal shocks and does not originate at the source. We calculate the expected degree of polarization for these two scenarios, and find that it is significantly easier to produce $P \gtrsim 50\%$ with an ordered field. More specifically, we obtain $P \sim 43\text{--}61\%$ for an ordered transverse magnetic field, B_{ord} , whereas a shock-produced field that is random but fully within the plane of the shock, B_{\perp} , can produce up to $P \lesssim 38\text{--}54\%$ for a single pulse in the GRB light curve, but the integrated emission over many pulses (as measured in GRB 021206) is expected to be a factor of ~ 2 lower. A magnetic field normal to the shock front, B_{\parallel} , can produce $P \sim 35\text{--}62\%$ for the emission integrated over many pulses. However, polarization measurements from GRB afterglows suggest a more isotropic configuration for the shock-produced field that should reduce P by a factor $\sim 2\text{--}3$. Therefore, an ordered magnetic field, B_{ord} , that originates at the source, can produce the observed polarization most naturally, while B_{\parallel} is less likely, and B_{\perp} is the least likely of the above.

Subject headings: gamma rays: bursts — polarization — shock waves — MHD

1. INTRODUCTION

The recent detection of a very large linear polarization, $P = 80\% \pm 20\%$, in the prompt γ -ray emission of GRB 021206 (Coburn & Boggs 2003, hereafter CB), establishes synchrotron emission as the dominant radiation mechanism in the prompt GRB. As the prompt GRB is believed to arise from internal shocks within a relativistic outflow (Rees & Mészáros 1994; Sari & Piran 1997), it can provide valuable information on the magnetic field structure in the ejecta, and clues to the nature of the central source. In a recent paper (Granot & Königl 2003, hereafter GK), we suggested that “the radiation from the original ejecta, which includes the prompt GRB and the emission from the reverse shock (the ‘optical flash’ and ‘radio flare’) could potentially exhibit a high degree of polarization (up to $\sim 60\%$) induced by an ordered transverse magnetic field advected from the central source”. This is perfectly consistent with the polarization measured in GRB 021206. CB also attributed the polarization in this GRB to an ordered magnetic field, and suggested that this implies that magnetic fields drive the GRB explosion. A similar interpretation of this measurement has even been claimed to favor Poynting dominated outflows in GRBs (Lyutikov, Periev & Blandford 2003).

However, Waxman (2003) suggested an alternative explanation: if the GRB outflow is a uniform jet with sharp edges and an opening angle $\theta_j \lesssim 1/\gamma$, then our line of sight is likely to be at an angle $\theta_j < \theta_{\text{obs}} \lesssim \theta_j + 1/\gamma$ from the jet axis. In this case we should see both a bright GRB (as much of the radiation is still beamed toward us) and a large polarization (e.g. Gruzinov 1999; Granot et al. 2002). This scenario does not require an ordered field and also works for a magnetic field that is generated at the internal shocks (Medvedev & Loeb 1999).

There are therefore two feasible explanations for the large polarization measured in GRB 021206, where only one of them requires a magnetic field ordered on angular scales $\gtrsim 1/\gamma$. This undermines the possible theoretical implications of an ordered magnetic field in the GRB ejecta. In this Letter we critically examine these two scenarios, and estimate their ability to explain the high observed polarization. In §2 we calculate the polarization from an ordered magnetic field. The maximal polarization for a narrow jet with a shock-produced magnetic field is calculated in §3. In §4 we apply our results to GRB 021206 and discuss the conclusions.

2. AN ORDERED MAGNETIC FIELD

Here we calculate the linear polarization for synchrotron emission from a thin spherical shell with an ordered transverse magnetic field, B_{ord} , moving radially outward with $\gamma \gg 1$. We integrate over the emission from the shell at a fixed radius and do not follow the different photon arrival times from different angles θ from the line of sight (l.o.s.). This calculation is relevant to the prompt GRB, the reverse shock (the ‘optical flash’ and ‘radio flare’) and the afterglow, provided the magnetic field is ordered over an angle $\gtrsim 1/\gamma$ around the l.o.s.

Following GK, the polarization position angle, measured from \hat{B}_{ord} , is given by $\theta_p = \phi + \arctan(\frac{1-y}{1+y} \cot \phi)$ in the limit $\gamma \gg 1$, where $y \equiv (\gamma\theta)^2$ and ϕ is the azimuthal angle. We have $I_{\nu} = I'_{\nu}(\nu/\nu')^3$, with¹ $I'_{\nu} \propto (\nu')^{-\alpha} (\sin \chi')^{\epsilon} \propto (\nu')^{-\alpha} [1 - (\hat{n}' \cdot \hat{B}'_{\text{ord}})^2]^{\epsilon/2}$, where $\nu/\nu' \approx 2\gamma/(1+y)$, $1 - (\hat{n}' \cdot \hat{B}'_{\text{ord}})^2 \approx$

¹ Here χ' is the angle between \hat{n}' and \hat{B}' , which is also the pitch angle between the electron’s velocity and \hat{B}' . For the optically thin part of the spectrum that is considered in this work, and as long as the electron energy distribution (taking into account electron cooling) is independent of the pitch angle χ' (which is most natural for a random field, and is also reasonable to expect, at least approximately, for an ordered field as well), we find $\epsilon = 1 + \alpha$.

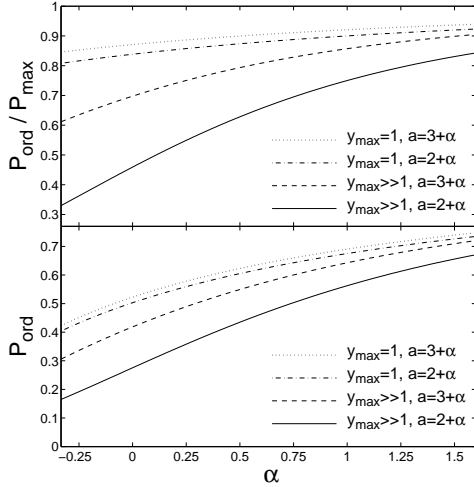


FIG. 1. — The polarization P_{ord} (lower panel) and $P_{\text{ord}}/P_{\text{max}}$ (upper panel) of synchrotron emission from an ordered transverse magnetic field, as a function of the spectral index α , for $\epsilon = 1 + \alpha$, calculated using Eq. (1).

$[(1-y)/(1+y)]^2 \cos^2 \phi + \sin^2 \phi$ and \hat{n}' is the direction in the local frame of a photon that reaches the observer. The Stokes parameters are given by

$$\frac{\begin{Bmatrix} U \\ Q \end{Bmatrix}}{IP_{\text{max}}} = \frac{\int \frac{dy}{(1+y)^a} \int d\phi \left[\left(\frac{1-y}{1+y} \right)^2 \cos^2 \phi + \sin^2 \phi \right]^{\epsilon/2} \begin{Bmatrix} \sin 2\theta_p \\ \cos 2\theta_p \end{Bmatrix}}{\int \frac{dy}{(1+y)^a} \int d\phi \left[\left(\frac{1-y}{1+y} \right)^2 \cos^2 \phi + \sin^2 \phi \right]^{\epsilon/2}}, \quad (1)$$

where $a = 3 + \alpha$ for the instantaneous emission (relevant for the afterglow) and $a = 2 + \alpha$ for the time integrated emission (relevant for the prompt GRB when integrated over a time larger than the duration of a single pulse, as in GRB 021206). For a uniform jet, the limits of integration should include only regions within the jet. This is important only if $\theta_{\text{obs}} + 1/\gamma \gtrsim \theta_j$, which is expected to be rare for the prompt GRB, but usually occurs during the afterglow. When the edge of the jet is at $y > y_{\text{max}} \gtrsim$ a few, the limits of integration may be taken as $\int_0^{y_{\text{max}}} dy \int_0^{2\pi} d\phi$. In this case $U = 0$ and $P_{\text{ord}} = -Q/I = |Q|/I$. For internal shocks, each pulse in the GRB light curve is from a collision between two shells. The emission near the peak of the pulse is mainly from $\theta \lesssim 1/\gamma$ ($y \lesssim 1$), and may be approximated by taking $y_{\text{max}} = 1$. The emission from $y \gtrsim 1$ contributes mainly to the tail of the pulse. If the latter is included in the temporal integration used for measuring P , and is not below the background, then we can take $y_{\text{max}} \gg 1$ (the asymptotic limit is reached at $y_{\text{max}} \gtrsim$ a few).

Figure 1 shows $P_{\text{ord}}/P_{\text{max}}$ and P_{ord} as a function of α for $\epsilon = 1 + \alpha$ (e.g. footnote 1), and Table 1 summarizes the results for the relevant (optically thin) power law segments (PLSs) of the spectrum.³

² Here $P_{\text{max}} = (\alpha + 1)/(\alpha + 5/3) = (p_{\text{eff}} + 1)/(p_{\text{eff}} + 7/3)$, where it is useful to define $p_{\text{eff}} \equiv 2\alpha + 1$. For optically thin synchrotron emission, $\alpha \geq -1/3$, and hence $P_{\text{max}} \geq 1/2$. This lower limit on P_{max} arises since $P = 1/2$ is simply the low frequency ($\nu \ll \nu_{\text{syn}}$) polarization of the synchrotron emission from each electron, and therefore $P_{\text{max}} = 1/2$ in PLSs D,E (see Table 1). For PLSs F, G and H, P_{max} is determined by $p_{\text{eff}} (= 2, p, \text{ and } p+1, \text{ respectively})$, where for these PLSs, p_{eff} is the effective power law index of the electron distribution.

³ The most relevant case for GRB 021206 is $y_{\text{max}} \gg 1$ and $a = 2 + \alpha$, for which the approximate formula $P_{\text{ord}}(\alpha) = 0.016\alpha^4 - 0.052\alpha^3 - 0.013\alpha^2 + 0.335\alpha + 0.276$, provides a relative accuracy of better than 0.25% for $-1/3 \leq$

TABLE 1. PARAMETER VALUES FOR DIFFERENT PLSs OF THE SPECTRUM

PLS	α	P_{max}	$P_{\text{ord}}(y_{\text{max}} = 1)$	$P_{\text{ord}}(y_{\text{max}} \gg 1)$
D, E	-1/3	1/2	0.404 (0.423)	0.165 (0.306)
F	1/2	9/13	0.605 (0.623)	0.435 (0.549)
G	$\frac{p-1}{2}$	$\frac{p+1}{p+7/3}$	0.605–0.675 (0.623–0.691)	0.435–0.563 (0.549–0.643)
H	$p/2$	$\frac{p+2}{p+10/3}$	0.675–0.726 (0.691–0.739)	0.563–0.656 (0.643–0.709)

NOTE. — Parameter values for different power law segments (PLSs) of the spectrum (that are labeled as in Granot & Sari 2002). Numerical values in PLSs G and H are for an electron index $2 < p < 3$. The values of P_{ord} without (with) parentheses are for $a = 2 + \alpha$ ($a = 3 + \alpha$) which are appropriate for the prompt GRB (afterglow). (see discussion below Eq. 1).

3. A VERY NARROW JET VIEWED FROM JUST OUTSIDE ITS EDGE

In this section we calculate the polarization from a narrow jet, of opening angle $\theta_j \sim 1/\gamma$, viewed at an angle $\theta_j \lesssim \theta_{\text{obs}} \lesssim \theta_j + 1/\gamma$ from its axis.⁴ In contrast to §2, here the magnetic field is assumed to be produced at the shock itself, and therefore has symmetry around the direction normal to the shock, \hat{n}_{sh} . Since the more isotropic the magnetic field configuration behind the shock, the lower the resulting polarization, we consider two extreme cases where the field is most anisotropic: 1. a random field that lies strictly within the plane of the shock ($B = B_{\perp}$, $P = P_{\perp}$), 2. a completely ordered field in the direction of \hat{n}_{sh} ($B = B_{\parallel}$, $P = P_{\parallel}$).

Following Ghisellini & Lazzati (1999), we generalize their formula so that it would hold for $\theta_{\text{obs}} > \theta_j$,

$$P = \frac{\frac{1}{2\pi} \int_{|\theta_j - \theta_{\text{obs}}|}^{\theta_j + \theta_{\text{obs}}} \theta d\theta I_{\nu}(\theta) P(\theta) \sin[2\psi_1(\theta)]}{\Theta(\theta_j - \theta_{\text{obs}}) \int_0^{\theta_j - \theta_{\text{obs}}} \theta d\theta I_{\nu}(\theta) + \int_{|\theta_j - \theta_{\text{obs}}|}^{\theta_j + \theta_{\text{obs}}} \theta d\theta \frac{\pi - \psi_1(\theta)}{\pi} I_{\nu}(\theta)}, \quad (2)$$

where $\cos \psi_1 = (\theta_j^2 - \theta_{\text{obs}}^2 - \theta^2)/2\theta_{\text{obs}}\theta$ and $\Theta(x)$ is the Heaviside step function. For B_{\parallel} we simply have $P_{\parallel}(\theta) = P_{\text{max}}$ and $\hat{n}' \cdot \hat{B}' = \hat{n}' \cdot \hat{r} = \cos \theta' \approx \frac{1-y}{1+y}$, so that $I_{\nu} \propto y^{\epsilon/2}/(1+y)^{3+\alpha+\epsilon}$. However, for B_{\perp} we must average over the possible field orientations within the plane of the shock:⁵

$$\frac{P_{\perp}(y)}{P_{\text{max}}} = \frac{\int_0^{\pi} d\phi \left[1 - \frac{4y \cos^2 \phi}{(1+y)^2} \right]^{(\epsilon-2)/2} \left[\left(\frac{1-y}{1+y} \right)^2 \cos^2 \phi - \sin^2 \phi \right]}{\int_0^{\pi} d\phi \left[1 - \frac{4y \cos^2 \phi}{(1+y)^2} \right]^{\epsilon/2}}, \quad (3)$$

and $I_{\nu} \propto (1+y)^{-3-\alpha}$ times the denominator of Eq. (3). For $\epsilon = 2$ and 0, $P_{\perp}(\theta')/P_{\text{max}} = \frac{-2y}{1+y^2} = \frac{-\sin^2 \theta'}{1+\cos^2 \theta'}$ and $-\min(y, 1/y)$, respectively. Fig. 2 shows $-P_{\perp}(\theta')/P_{\text{max}}$ for several values of ϵ . A larger ϵ implies a larger $|P(\theta')|$, as it suppresses I_{ν} at $(\hat{n}' \cdot \hat{B}')^2 \approx 1$ where there is a positive contribution to $P_{\perp}(\theta')$.

$\alpha \leq 3/2$.

⁴ It is assumed here that the jet has sharp edges, i.e. the emissivity drops sharply over an angular interval $\Delta\theta \ll 1/\gamma$ around $\theta = \theta_j$. A smoother edge, $\Delta\theta \gtrsim 1/\gamma$, would considerably reduce the polarization.

⁵ Here $P < 0$ ($P > 0$) implies \hat{P} along (perpendicular to) the plane containing \hat{n}_{sh} and \hat{n}' .

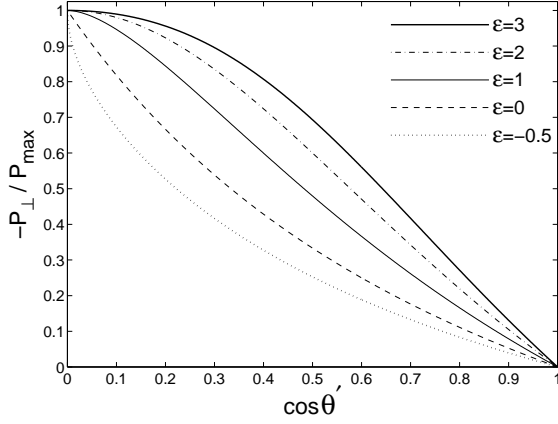


FIG. 2.— The local polarization, $|P_{\perp}(\theta')| = -P_{\perp}(\theta')$, normalized by P_{\max} , for a magnetic field that is fully tangled within a plane, and emission at an angle θ' from the normal to the plane, for $\epsilon = -0.5, 0, 1, 2, 3$.

The global polarization from the whole jet is given by⁶

$$\frac{P_{\parallel}}{P_{\max}} = \frac{\frac{1}{2\pi} \int_{y_1}^{y_2} \frac{y^{\epsilon/2} dy}{(1+y)^{\epsilon+1}} \sin[2\psi_1(y)]}{\Theta(1-q) \int_0^{y_1} \frac{y^{\epsilon/2} dy}{(1+y)^{\epsilon+1}} + \int_{y_1}^{y_2} \frac{y^{\epsilon/2} dy}{(1+y)^{\epsilon+1}} \frac{[\pi - \psi_1(y)]}{\pi}}, \quad (4)$$

$$\frac{P_{\perp}}{P_{\max}} = \frac{\frac{1}{2\pi} \int_{y_1}^{y_2} \frac{dy \sin[2\psi_1(y)]}{(1+y)^{\epsilon}} g(y, \epsilon)}{\Theta(1-q) \int_0^{y_1} \frac{f(y, \epsilon) dy}{(1+y)^{\epsilon}} + \int_{y_1}^{y_2} \frac{f(y, \epsilon) dy}{(1+y)^{\epsilon}} \frac{[\pi - \psi_1(y)]}{\pi}}, \quad (5)$$

$$f(y, \epsilon) = \int_0^{\pi} d\phi \left[1 - \frac{4y \cos^2 \phi}{(1+y)^2} \right]^{\epsilon/2}, \quad (6)$$

$$g(y, \epsilon) = \int_0^{\pi} d\phi \frac{(1-y)^2 (1+y)^{-2} \cos^2 \phi - \sin^2 \phi}{[1 - 4y(1+y)^{-2} \cos^2 \phi]^{(2-\epsilon)/2}}, \quad (7)$$

where $\cos \psi_1 = [(1-q^2)y_j - y]/(2q\sqrt{y_j y})$, $q \equiv \theta_{\text{obs}}/\theta_j$, $y_j = (\gamma\theta_j)^2$, $y_1 = (1-q)^2 y_j$, $y_2 = (1+q)^2 y_j$.

Figures 3 and 4 show $P_{\perp}(q)$ and $P_{\parallel}(q)$, respectively, for several values of α and y_j , using the relation $\epsilon = 1 + \alpha$. For $q < 1$, $|P_{\perp}|/P_{\max} \lesssim 0.2$, while $|P_{\perp}|$ rises sharply above $q = 1$ (the larger y_j , the sharper the rise), and peaks at $q \sim 1 + 1/\sqrt{y_j}$ ($q \approx 1.7-1.8$ for $y_j = 1$), which is q just above 1 for $y_j \gg 1$, but at $q \sim 1/\sqrt{y_j} \gg 1$ for $y_j \ll 1$. The width of the peak is $\sim 1/\sqrt{y_j}$, so that the peak is wider (as well as higher) for smaller y_j . At larger values of q , $|P_{\perp}|$ decreases since for $\theta_{\text{obs}} \gtrsim (2-3)\max(\theta_j, 1/\gamma)$ [i.e. $q \gtrsim (2-3)\max(1, 1/\sqrt{y_j})$], the jet may be approximated as a point source, and as q increases, the emission in the local frame is almost straight backward (i.e. \hat{n}' approaches $-\hat{n}_{\text{sh}}$ and θ' approaches π), thus suppressing $P_{\perp}(\theta')$ (see Fig. 2). However, in sharp contrast with B_{\perp} , for B_{\parallel} even if θ' is only slightly different from π , still $P_{\parallel}(\theta') = P_{\max}$, and P_{\parallel} approaches P_{\max} for $q \gtrsim 2$. The transition between $P_{\parallel}(q \gtrsim 2) \approx P_{\max}$ and $P_{\parallel}(q = 0) = 0$ is very gradual for $y_j \ll 1$ and very sharp for $y_j \gg 1$ (for which the transition occurs at $|q-1| \lesssim y_j^{-1/2} \ll 1$). For $y_j > 1$, $P_{\parallel}(q < 1)/P_{\max} \lesssim 0.3$, which is a little higher than $|P_{\perp}|$, while for $y_j < 1$, $P_{\parallel}(q < 1)/P_{\max} \lesssim 0.6$. For $y_j \gg 1$ ($\theta_j \gg 1/\gamma$) the edge of the jet is hardly visible from the interior of the jet and $P(q < 1 - 1/\sqrt{y_j}) \approx 0$ (for both B_{\perp} and B_{\parallel}).

The above expressions for $P_{\perp}(q, y_j, \epsilon, a)$ or $P_{\parallel}(q, y_j, \epsilon, a)$ can produce afterglow polarization light curves, by using $a = 3 + \alpha$,

⁶ Here, $P < 0$ ($P > 0$) means \hat{P} along (perpendicular to) the direction from our l.o.s. to the jet axis.

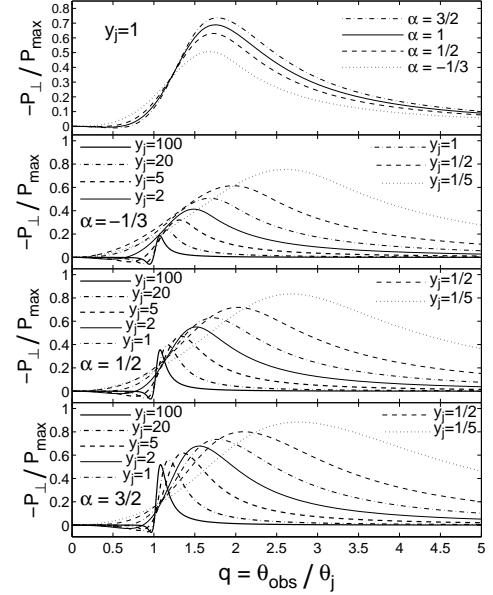


FIG. 3.— The polarization $-P_{\perp}(q)/P_{\max}$ for several values of α and y_j , calculated using Eq. (5) with $a = 2 + \alpha$ and $\epsilon = 1 + \alpha$.

$\epsilon = 1 + \alpha$ and $P_{\max} = \frac{\alpha+1}{\alpha+5/3}$, and adding a model for the time evolution of $\gamma(t)$ and $\theta_j(t)$, which determine $q(t) = \theta_{\text{obs}}/\theta_j(t)$ and $y_j(t) = [\gamma(t)\theta_j(t)]^2$. One simple model is to assume $q(t < t_j), y_j(t > t_j) = \text{const}$, where t_j is the jet break time.⁷ Note that at a fixed observed time, P remains constant within each PLS, but changes across spectral breaks.

4. APPLICATION TO GRB 021206 AND DISCUSSION

In the prompt GRB the spectral index is usually in the range $1/2 \lesssim \alpha \lesssim 5/4$, for which the time integrated polarization ($a = 2 + \alpha$, $y_{\text{max}} \gg 1$) from an ordered transverse magnetic field (B_{ord}) is $P_{\text{ord}} \sim 43-61\%$ (e.g. Table 1, Fig. 1, footnote 3). This is reasonably consistent with the value of $P = 80\% \pm 20\%$ that was measured for GRB 021206 (CB). Furthermore, this requires a magnetic field that is ordered over angles $\gtrsim 1/\gamma$ which can still be $\ll \theta_j$.

We now turn to the narrow jet scenario (Waxman 2003). For $\theta_{\text{obs}} > \theta_j + 1/\gamma$ the observed flux from the GRB drops considerably. Therefore, a bright GRB like 021206 requires $q \lesssim 1 + 1/\sqrt{y_j}$. As it is hard to collimate a jet to $\theta_j < 1/\gamma$, it is reasonable to assume $y_j \gtrsim 1$ and therefore $q \lesssim 2$. Furthermore, for $y_j \gg 1$ that is usually inferred from afterglow observations (Panaitescu & Kumar 2002), the peak of the polarization is at $q \sim 1 + 1/\sqrt{y_j} \sim 1$ and has a width $\Delta q \sim 1/\sqrt{y_j} \ll 1$ which covers a fraction $\sim 1/\sqrt{y_j} \ll 1$ of the solid angle from which the GRB is beamed toward us, and therefore a high polarization is very unlikely. Hence, we require $y_j \lesssim 2$. The fact that GRB 021206 was extraordinarily bright, together with the correlation found by Frail et al. (2001), might suggest a very narrow jet, so that $y_j \lesssim 2$ is not so far fetched (Waxman 2003). Altogether we expect $1 \lesssim y_j \lesssim 2$ and $1 \lesssim q \lesssim 2$.

In this parameter range, and for $1/2 \lesssim \alpha \lesssim 5/4$, P_{\perp} peaks at $P_{\perp, \text{max}} \sim (0.55-0.7)P_{\max} \sim 38-54\%$. However, the Lorentz

⁷ Ghisellini & Lazzati (1999) simply assumed $\theta_j, \alpha = \text{const}$, and implicitly assumed $\epsilon = 2$ since they used $P(\theta')/P_{\max} = \sin^2 \theta' / (1 + \cos^2 \theta')$. However, they did not take into account the fact that $I'_{\nu} \propto \langle (\sin \chi')^{\epsilon} \rangle \propto \langle [1 - (\hat{B}' \cdot \hat{n}')^2]^{\epsilon/2} \rangle$, which effects the polarization light curves.

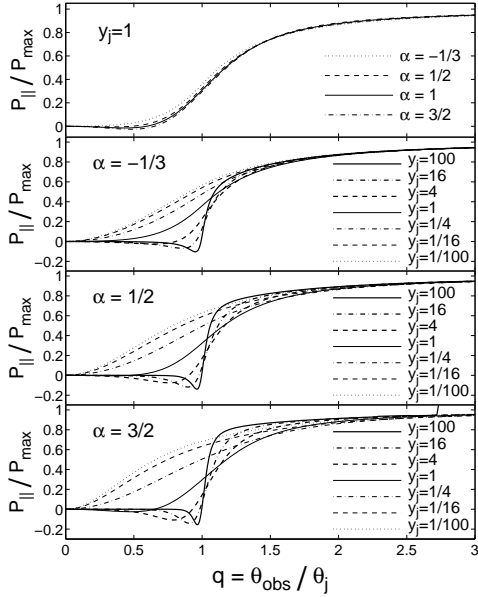


FIG. 4.— The same as Fig. 3 but for P_{\parallel} using Eq. (4).

factor of the shocked fluid in the internal shocks is expected to vary with $\Delta\gamma \sim \gamma$ between different shell collisions within the same GRB.⁸ This implies a reasonably large variation in $y_j \propto \gamma^2$, while $q = \text{const}$, so that our l.o.s. will not be near the peak of P_{\perp} for all the pulses in the GRB light curve. Furthermore, the observed flux at $q \sim 1 + 1/\sqrt{y_j}$, where P_{\perp} peaks, is smaller than near the edge of the jet ($q \approx 1$), due to relativistic beaming effects, so that the brightest pulses would tend to be relatively weakly polarized, thus further reducing the average polarization over the whole GRB. Therefore, while for a single pulse in the GRB light curve P_{\perp} can approach $P_{\perp, \text{max}}$, the average over many pulses (as in GRB 021206) will be $P_{\perp} \lesssim P_{\perp, \text{max}}/2 \sim 19\text{--}27\%$.

For B_{\parallel} we find $P_{\parallel} \sim (0.3\text{--}0.9)P_{\text{max}} \sim 20\text{--}70\%$ for a single pulse, and expect $P_{\parallel} \sim (0.5\text{--}0.8)P_{\text{max}} \sim 35\text{--}62\%$ for the average over many pulses, which is consistent with the value

⁸ If B_{ord} is ordered on angles $\gtrsim 1/\gamma_{\text{min}}$, which are still $\lesssim 0.01$, and \hat{B}_{ord} does not change significantly (i.e. by $\lesssim 0.5$ radians) between the different shells, then this should not effect P_{ord} significantly; P_{\parallel} should also not be strongly effected.

⁹ except for a possible sharp spike with $P \approx 10\%$ in the polarization light

measured for GRB 021206. In fact, B_{\parallel} is an ordered magnetic field, just that unlike B_{ord} which was considered in §2, it can in principle be generated at the shock itself, as \hat{n}_{sh} is a preferred direction that is determined locally by the shock front. Current models for the production of magnetic fields at collisionless relativistic shocks (Medvedev & Loeb 1999) suggest $B = B_{\perp}$ rather than B_{\parallel} . However the amplification mechanism of the magnetic field and its configuration in relativistic shocks is still largely an open question, so that it is hard to rule out $B \approx B_{\parallel}$ on purely theoretical grounds. Nevertheless, it is important to keep in mind that we considered two extreme cases for the magnetic field configuration behind the shock, in which it is most anisotropic. The relatively low values of $P \lesssim 3\%$ measured in GRB afterglows⁹, compared to the expected values of $P \lesssim 20\%$ (Sari 1999; Ghisellini & Lazzati 1999; GK), suggest that the magnetic field created behind relativistic shocks is more isotropic than the extreme cases we considered, implying P values lower by a factor of $\sim 2\text{--}3$ (e.g. GK). Therefore, although $P_{\parallel} \sim 35\text{--}62\%$, a more isotropic magnetic field configuration that is suggested by afterglow observations would imply¹⁰ $P \sim 15\text{--}30\%$.

We therefore conclude that $P \gtrsim 50\%$ is most naturally produced by an ordered magnetic field that is carried out with the ejecta from the central source (as was recently proposed by GK). This is therefore the most likely explanation for the value of $P = 80\% \pm 20\%$ (CB) measured in GRB 021206. A magnetic field that is generated at the shock itself is less likely to produce a sufficiently large polarization. However, if either 1) the systematic uncertainty in the quoted value was for some reason underestimated, and $P \lesssim 20\text{--}30\%$ is acceptable, or 2) the internal shocks for some reason produce a magnetic field much more anisotropic than in the afterglow shock, then P_{\parallel} may still be a viable option. Both points are required in order for P_{\perp} to work well.

I thank Davide Lazzati, Arieh Königl, Ehud Nakar and Eli Waxman for useful discussions. This research was supported by the Institute for Advanced Study, funds for natural sciences.

curve of GRB 020405 (Bersier et al. 2003).

¹⁰ The same argument should reduce $P_{\perp} \sim 19\text{--}27\%$ to $P \sim 7\text{--}13\%$, making it even harder to reconcile with the value measured in GRB 021206.

REFERENCES

- Bersier, D., et al. 2003, ApJ, 583, L63
 Coburn, W., & Boggs, S.E. 2003, Nature, 423, 415
 Frail, D. A., et al. 2001, ApJ, 562, L55
 Ghisellini, G., & Lazzati, D. 1999, MNRAS, 309, L7
 Granot, J., & Königl, A. 2003, ApJ, 594, L83 (GK)
 Granot, J., Panaitescu, A., Kumar, P., & Woosley, S. E. 2002, ApJ, 570, L61
 Granot, J., & Sari, R. 2002, ApJ, 568, 820
 Gruzinov, A. 1999, ApJ, 525, L29
 Lyutikov, M., Pariev, V. I., & Blandford, R. D. 2003, ApJ, in press (astro-ph/0305410)
 Medvedev, M. V., & Loeb, A. 1999, ApJ, 526, 697
 Panaitescu, A., & Kumar, P. 2002, ApJ, 571, 779
 Rees, M. J., & Mészáros, P. 1994, ApJ, 430, L93
 Sari, R., & Piran, T. 1997, ApJ, 485, 270
 Sari, R. 1999, ApJ, 524, L43
 Waxman, E. 2003, Nature, 423, 388